Arch. Metall. Mater. **68** (2023), 4, 1369-1375

DOI: https://doi.org/10.24425/amm.2023.146202

P. KALIUZHNYI[1*], I. SHALEVSKA[1], V. SLIUSAREV[1]

MICROSTRUCTURE OF REINFORCED CAST IRON PRODUCED BY LOST FOAM CASTING

The article considers the method of obtaining reinforced castings from gray cast iron by lost foam casting. The aim of this study was to determine the microstructure formation of gray cast iron reinforced with inserts of carbon and stainless steel in this casting method. The results of the research have shown that the products of destruction of expanded polystyrene have a positive effect on the bonding formation of cast iron with reinforcing inserts. When steel wire is used as reinforcement, a decarbonized layer of cast iron is being formed around it, in which the inclusions of graphite are smaller and their quantity is less than in the main metal. Due to carburization, the surface structure of the reinforcement changes from ferrite to pearlite with cementite. Steel wire reinforcement can be effective in increasing strength and toughness of gray cast iron. The usage of stainless steel reinforcement leads to the formation of a transition layer on the part of the matrix metal. It contains ledeburite with dissolved chromium, which increase the wear resistance of cast iron.

Keywords: Gray cast iron; Reinforcement; Microstructure; Lost foam casting

1. Introduction

Cast composite products are increasingly used in various industries. The combination in one part of different properties allows increasing its resource efficiency. To obtain composite parts of complex configuration, the most rational is using of casting technology as cast blanks require minimal machining. The manufacture of high-precision cast products of complex geometry, including composite and bimetallic castings, is advisable to carry out by lost foam casting (LFC). Currently, there are examples of obtaining composite castings by solid-liquid combination by LFC method from Al/Cu [1,2], Al/steel [3], Mg/Al [4,5], cast iron/Cu [6] etc. In most cases, the solid-liquid combination of reinforcing inserts (rods, wire) are fixed in a polystyrene pattern, which during pouring the matrix alloy is destructed under the action of its heat, or glued to the surface of the foam pattern (plate). There are also examples of obtaining bimetallic castings by liquid-liquid combination of two different aluminum alloys [7] or chromium white cast iron with carbon steel [8]. In the case of liquid-liquid combination, the alloys are either successively poured (through two different gating systems) into the mold, or simultaneously. However, in the last case, the alloys can be mixed so partitions can be used to prevent this [9].

From a practical point of view, the properties of the composite and their level are important. From a scientific point of view, the processes that occur when the matrix metal interacts with the reinforcing elements represent particular interest because they determine the quality of the joining which directly affects the properties of the composite. Numerous studies show that the nature of the interaction is influenced by the following factors: the type of alloy (material) of the matrix and reinforcement, pouring temperature, the ratio of their masses or volumes, the geometric dimensions of the reinforcement, etc.

Gray cast iron is a versatile construction material for various cast parts due to its good casting properties, good machinability and low cost. However, it has low mechanical properties. Therefore, research aimed at increasing, first of all, the strength and toughness of gray cast iron by introducing reinforcing inserts from materials with higher data characteristics is relevant.

There are studies [10,11] of composite castings made of gray cast iron reinforced with steel wire which showed that its strength and toughness can be increased by 30% and 40%, respectively. Reinforcement with low-carbon plates increased the toughness of gray cast iron by 5-15% [12]. Studies of castings obtained by pouring gray cast iron on stainless steel plates [13,14] have shown that such bimetallic castings had a high quality of metal bonding and a functional wear-resistant working layer

[1] DEPARTMENT OF PHYSICAL CHEMISTRY OF FOUNDRY PROCESSES, PHYSICO-TECHNOLOGICAL INSTITUTE OF METALS AND ALLOYS OF THE NATIONAL ACADEMY OF SCIENCES OF UKRAINE, UKRAINE

* Corresponding author: kpb.ptima@gmail.com

was formed on the plate side. However, the gray cast iron composite and bimetallic castings mentioned above were obtained by casting into conventional sand molds.

In LFC technic during metal pouring, which is accompanied by the destruction of the expanded polystyrene (EPS) pattern, the reinforcing elements are wetted with liquid products of the destruction of EPS and the formation of reducing atmosphere in the melt-pattern gap. All these facts can affect the interaction of the matrix melt with the reinforcement. Since the physical, mechanical and service properties of cast iron are determined primarily by the peculiarities of its microstructure, this study was dedicated to the microstructure formation of reinforced gray cast iron castings made by LFC.

2. Experimental

Disposable patterns were made of EPS with a density of 20 kg/m^3 in the form of plates 200×100×15 mm. Reinforcing inserts with a diameter of 1, 2, 3 and 4 mm and the length of 230 mm were placed longitudinally in them (Fig. 1a). Wire of galvanized steel EN 1.0402 and wire rope 7×7 of stainless steel EN 1.4301 were used as such inserts, the chemical composition of which is given in TABLE 1. The PolySpek Junior spectrometer was used for chemical analysis of the materials. Experimental plan is presented in TABLE 2.

The gates and the riser were glued to the EPS patterns after which the refractory paint was applied. After drying the coating, the pattern block was molded in dry silica sand compacting with vibration. The molds were filled with gray cast iron EN-GJL-250 (TABLE 1) at the temperature of 1400°C and a vacuum value of 0.04 MPa in sand. Samples for metallographic study were cut from the obtained castings (Fig. 1b). The shape and distribution of graphite inclusions in cast iron were studied on unetched sections. The samples were etched with picral agent to detect the structure of the metal matrix of cast iron and reinforcement. Metallographic studies were performed using optical microscope and Tescan Vega 3 SEM with a Bruker EDX attachment to determine the local chemical analysis of the phases.

TABLE 1

Chemical composition of materials, wt. %

Material	C	Si	Mn	P	S	Cr	Ni	Fe
EN-GJL-250	3.2	1.8	0.7	0.05	0.03	—	—	Bal.
EN 1.0402	0.2	0.2	0.5	0.02	0.02	—	—	Bal.
EN 1.4301	0.06	0.6	1.7	0.02	0.015	18.0	10.0	Bal.

TABLE 2

Experimental plan

Reinforcing insert		Diameter, mm			
Material	Form	1	2	3	4
EN 1.0402	Wire	+	+	+	+
EN 1.4301	Wire rope	+	+	–	+

3. Results and discussion

Studies of control samples of unreinforced gray cast iron have shown that in its structure there is lamellar graphite of form I with uniform distribution A (ISO 945-1: 2019) (Fig. 2a). The length of graphite inclusions is 60-120 μm. The metal matrix of unreinforced cast iron is pearlitic with a small (up to 5%) content of ferrite without cementite (Fig. 2b).

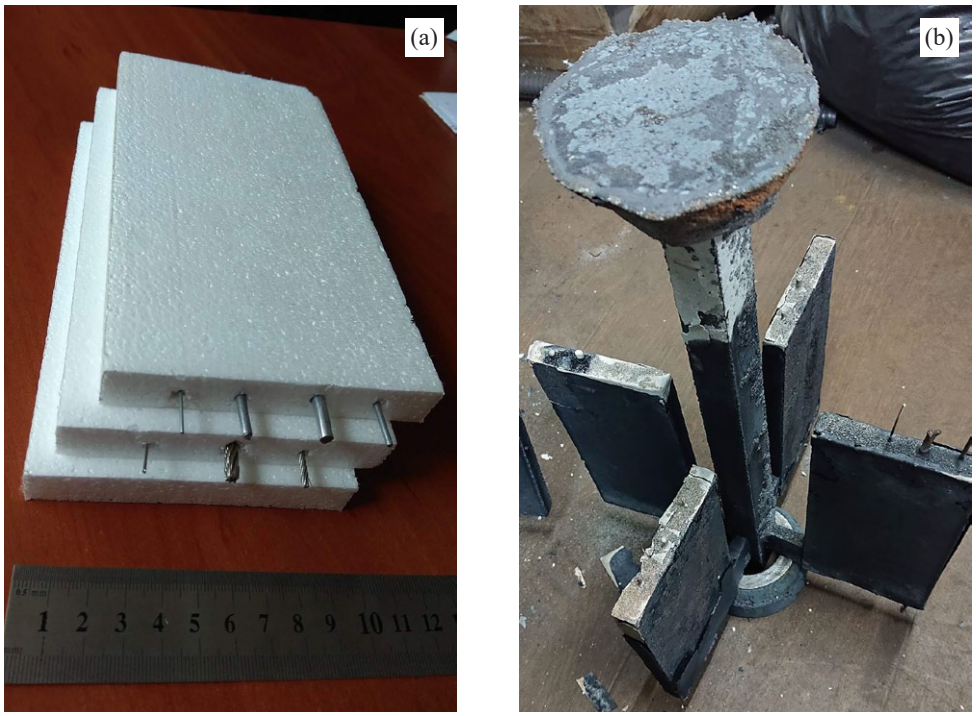

Fig. 1. EPS patterns with reinforcement (a) and castings (b)

The study of reinforced cast iron samples showed that inserts with the diameter of 1 mm made of carbon and stainless steel were completely melted and were not visually identified in the structure of the samples. In all other studied samples, perfect bonding of gray cast iron with reinforcing inserts was observed.

Studies of unetched samples with carbon steel reinforcements with diameters of 2, 3 and 4 mm showed that there are graphite inclusions of form I distribution D (ISO 945-1: 2019) around the inserts and they are smaller (15-30 μm) than the base metal (Fig. 3). Obviously, this is due to the faster rate of crystallization of local volumes of cast iron because of the cooling action of the reinforcements. Also the number of graphite inclusions around the steel inserts is less than in the main metal, due to the decarburization of cast iron, which causes a decrease in carbon emissions in free form.

Graphite form I distribution D (ISO 945-1: 2019) with a particle size of 15-30 μm is observed around the inserts in samples with stainless steel reinforcements (Fig. 4). However, the area

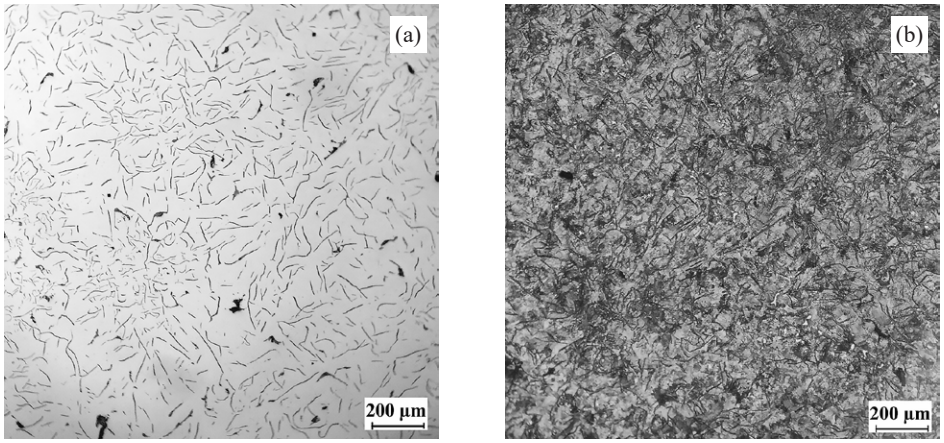

Fig. 2. Microstructure of unetched (a) and etched (b) unreinforced gray cast iron

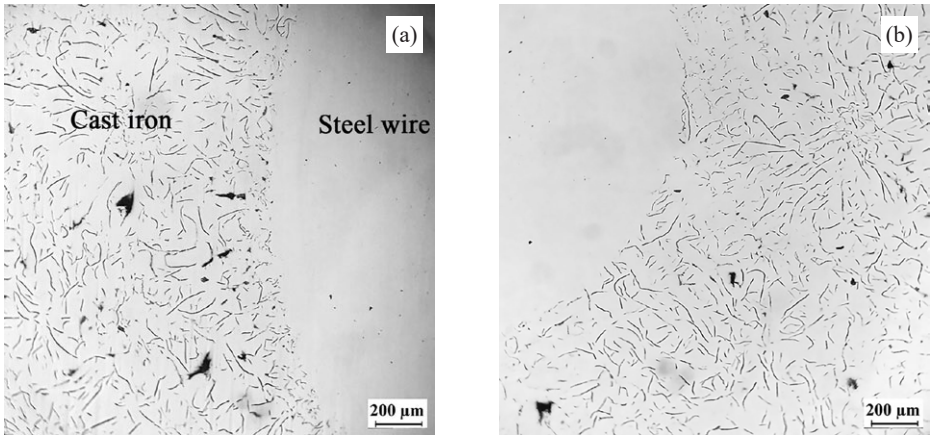

Fig. 3. Microstructure of cast iron with carbon steel wire Ø 4 mm (a) and Ø 2 mm (b)

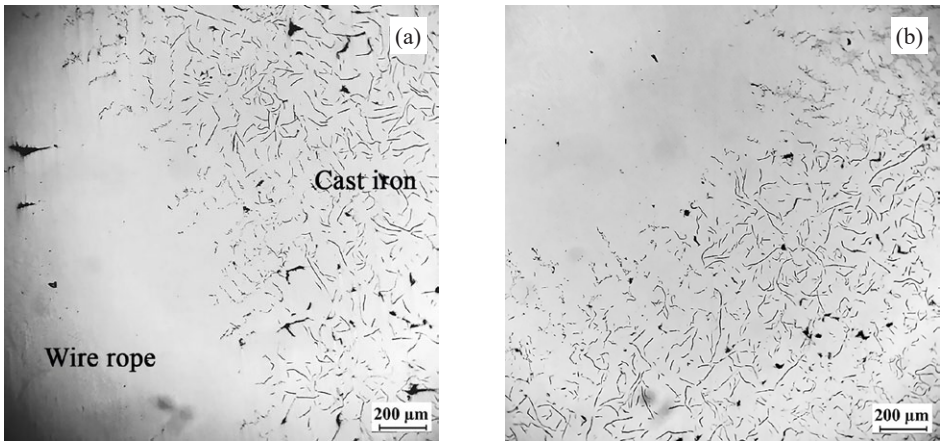

Fig. 4. Microstructure of cast iron with stainless steel inserts Ø 4 mm (a) and Ø 2 mm (b)

depleted of graphite inclusions extends to a greater depth from the insert surface compared to samples of cast iron reinforced with carbon steel wire.

The microstructure of etched samples of reinforced cast iron in the case of steel wire with the diameter of 2, 3 and 4 mm is similar (Fig. 5). There is a decarbonized layer of cast iron (region I) with a thickness of 0.1-0.2 mm around the steel inserts, which is formed due to the diffusion of carbon from cast iron to steel owing to their significant difference in content in the matrix alloy and reinforcement. It also leads to the change in the structure of steel reinforcement – the central part of the reinforcement remains ferrite with a small amount of perlite, the structure changes to pearlite (region III) with the approach to the interface, and pearlite with cementite mesh (region II) is near the surface.

In samples with wires with the diameter of 3 and 4 mm, the thickness of the carburized layer is 0.40-0.45 mm, 0.18-0.23 mm of which is the pearlitic zone with cementite mesh. In the case of wire with a diameter of 2 mm, the pearlite zone with cementite mesh is 0.25-0.30 mm, and the total thickness of the carburized layer is 0.46-0.51 mm. That is, the carburization of 2 mm wire is greater than 3 and 4 mm wire. 2 mm wire cools the matrix metal less due to the smaller thickness and smaller mass, and therefore the system is longer at the temperature at which the active diffusion of carbon occurs.

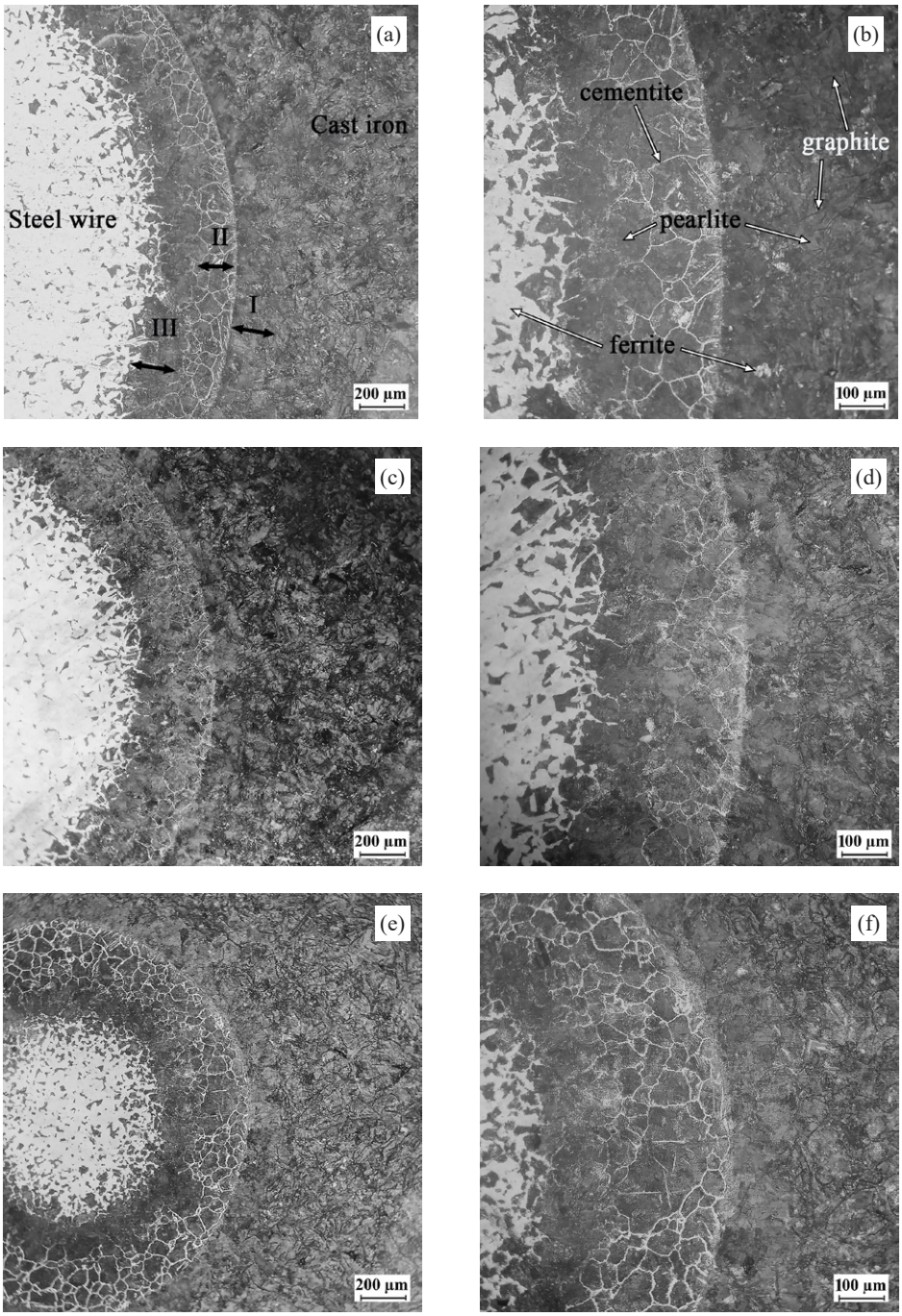

Fig. 5. Microstructure of the bonding zone of gray cast iron with steel wire Ø 4 mm (a, b), Ø 3 mm (c, d) and Ø 2 mm (e, f)

Fig. 6 shows the microstructure of cast iron, which is reinforced with stainless steel wire rope Ø 4 mm and Ø 2 mm, after etching. The structure of the reinforcement in the center remains austenitic, and in the near-surface local areas appear chromium carbides due to carburization. The presence of chromium carbides, which reduce the corrosion resistance of austenitic steel, can be judged by the effects of etching of metallographic samples [15].

Fig. 6(a) shows that the extreme fibers of the rope partially dissolved in the matrix alloy which led to the formation of a wide transition zone. The thickness of such transition layer is 0.8-1.1 mm in the case of Ø 4 mm and Ø 2 mm inserts. The microstructure of the transition zone was studied in more detail using a scanning electron microscope. SEM microstructures are shown in Fig. 7. Results of chemical EDX analysis of the points are marked in Fig. 7, given in TABLE 3.

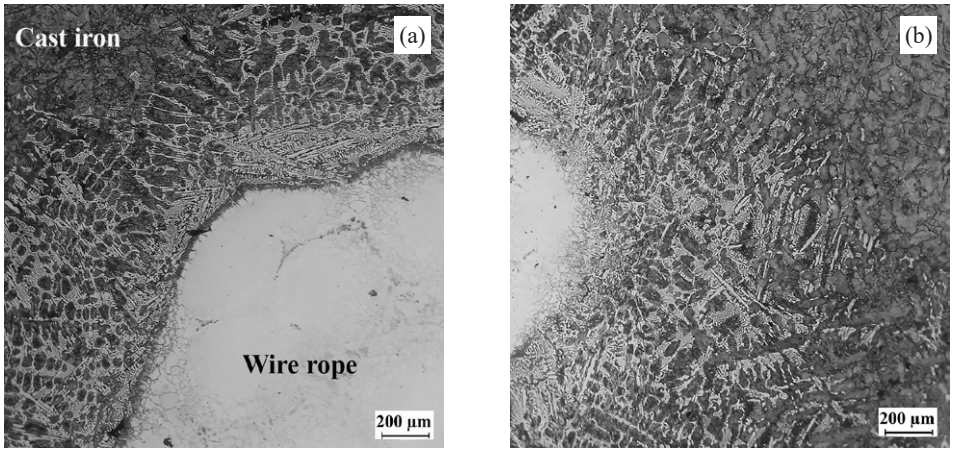

Fig. 6. Microstructure of the transition zone between gray cast iron and stainless steel inserts Ø 4 mm (a) and Ø 2 mm (b)

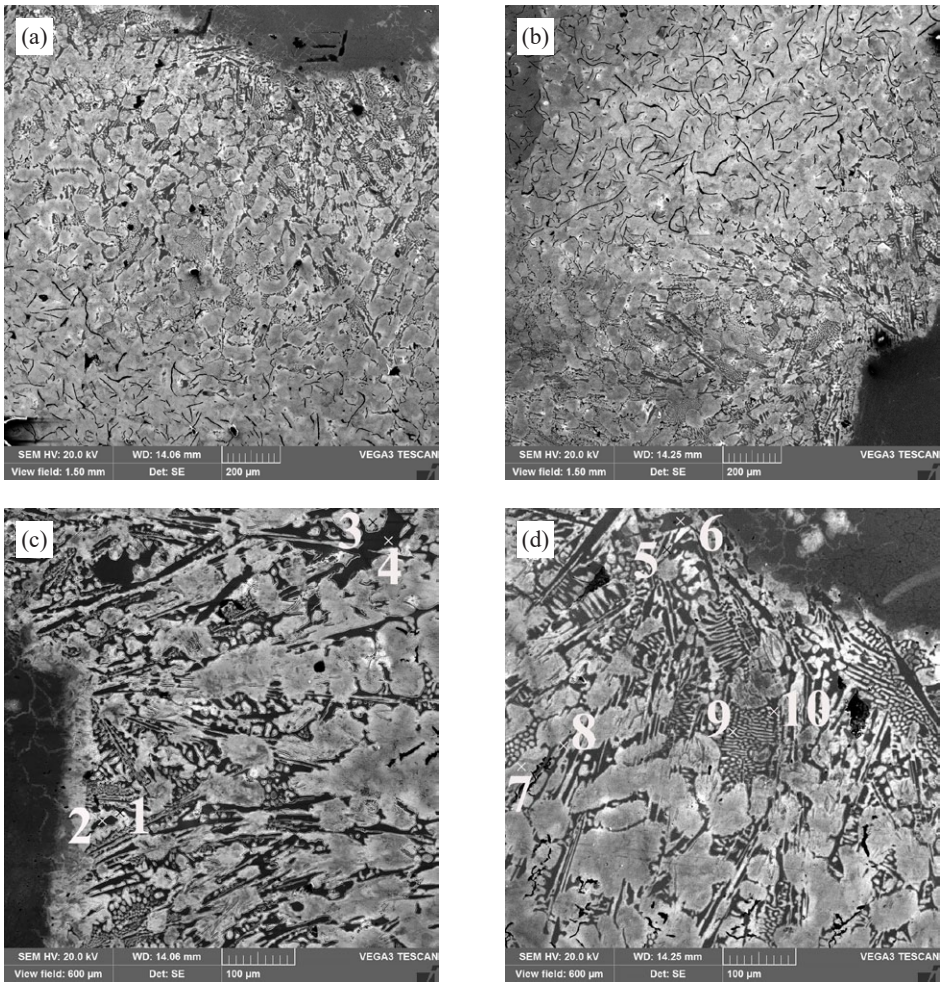

Fig. 7. SEM microstructure of the transition zone between gray cast iron and stainless steel inserts Ø 4 mm (a, c) and Ø 2 mm (b, d)

TABLE 3

The result of EDX analysis in points from Fig. 7

No. of point	Element	C	Si	Mn	Cr	Ni	Fe
1	Mass. %	5.28	1.81	0.63	2.22	1.78	87.81
	At. %	20.30	2.97	0.53	1.97	1.40	72.60
2	Mass. %	5.36	0.05	0.96	6.30	0.49	85.35
	At. %	20.85	0.09	0.82	5.67	0.39	71.46
3	Mass. %	4.08	1.68	0.51	1.06	0.74	91.87
	At. %	16.28	2.87	0.45	0.98	0.61	78.79
4	Mass. %	5.41	0.07	0.8	3.61	0.22	89.66
	At. %	20.95	0.12	0.68	3.23	0.18	74.73
5	Mass. %	4.16	1.83	0.45	2.32	2.50	88.74
	At. %	16.54	3.11	0.39	2.13	2.03	75.81
6	Mass. %	4.94	0.05	0.63	11.06	0.63	82.70
	At. %	19.33	0.08	0.50	9.99	0.50	69.56
7	Mass. %	3.24	1.68	0.37	0.52	0.34	93.86
	At. %	13.26	2.94	0.33	0.49	0.28	82.69
8	Mass. %	5.03	0.03	0.63	4.90	0.25	89.15
	At. %	19.68	0.06	0.54	4.43	0.20	75.08
9	Mass. %	3.57	2.45	0.40	1.20	2.88	90.10
	At. %	14.39	4.23	0.35	1.12	1.88	78.05
10	Mass. %	5.16	0.20	0.70	4.05	0.70	89.19
	At. %	20.11	0.33	0.60	3.65	0.56	74.46

The transition zone consists of pearlite, ledeburite and carbides. Perlite contains Cr and Ni in addition to Si and Mn. At a distance of 50 μm from the border of the reinforcement, pearlite contains 2.5% wt. Cr and Ni (points 1 and 5, Fig. 7). The amount of Cr and Ni decreases (points 3 and 7) with distance from the reinforcement.

In the structure of the transition layer, honeycomb ledeburite is distinguished which consists of pearlite (point 9) and chromium-doped cementite (point 10, Fig. 7). The analysis shows that the carbides in the transition layer are cementite, which is alloyed with chromium. It is known from the literature that Cr can dissolve in cementite up to 20%. From 3.6% of Cr (point 4) to 11% (point 6) dissolves in these carbides. The presence of carbides in the structure of reinforced cast iron leads to an increase in its wear resistance while the strength and toughness are reduced.

Wire-type inserts interact more intensively with cast iron than stainless steel plates [13,15]. The nature of the interaction is influenced by the fact that the wire is surrounded on all sides by cast iron, i.e. it warms up better and has a larger surface area for chemical interaction. Wire reinforcement causes a stronger interaction compared to stainless steel plates [16]. Accordingly, the thickness of the transition layer, including the newly formed carbides, is greater.

The intensification of heat and mass transfer processes is also influenced by the ratio of the masses of the casting and reinforcement. The significant advantage of the mass of cast iron over the mass of the inserts helps to increase the intensity of heat and mass transfer processes in the transition zone and increase the values of the effective diffusion coefficients of chemical elements. The fibers of the wire rope are more affected by the matrix metal due to their small thickness, which as a result creates conditions for more intensive interfacial interaction.

The presence of a dense diffusion layer indicates a positive effect of the destruction products of EPS on the formation of the joining between the reinforcement and the matrix alloy, and in general the suitability of the LFC method to obtain such cast composites. In addition, the formation of joining between the reinforcement and the matrix alloy is influenced by the amount of vacuum in the mold. Depending on the amount of vacuum, the front of metal interaction with the pattern takes a different configuration [5], which can either contribute to the targeted removal of polystyrene degradation products through refractory coating or their delay on the reinforcement surface and the formation of defects in the casting. The presence in the pattern of reinforcing elements oriented along the direction of movement of the melt during the pouring of the alloy under vacuum creates conditions for leveling the metal front, which helps to remove the gases from the metal [17].

4. Conclusions

Composite cast iron castings with carbon and stainless steel reinforcement have been successfully fabricated by LFC. When gray iron interacts with steel wire, a homogeneous transition layer is formed, the formation of which occurs owing to the diffusion of carbon. A thicker transition layer is formed without a clear interface between dissimilar metals when gray cast iron interacts with stainless steel. The microstructure of the transition layer differs from the structure of the matrix alloy and the structure of the reinforcing metal and consists of pearlite doped with Cr and Ni and cementite doped with Cr. The formation of the microstructure and the size of the transition zone are influenced by the chemical composition of the matrix alloy and reinforce-

ment, the temperature of the liquid matrix alloy and the cooling rate of the casting, which is also associated with the amount of reinforcing metal and its shape.

REFERENCES

[1] S. Acar, R. Gecü, A. Kisasöz, K.A. Güler, A. Karaaslan, Pract. Metallogr. **55** (11), 728-740 (2018).

[2] F. Guan, W. Jiang, G. Li, H. Jiang, J. Zhu, Z. Fan, Mater. Res. Express. **6** (9), 096529 (2019).

[3] K.H. Choe, K.S. Park, B.H. Kang, G.S. Cho, K.Y. Kim, K.W. Lee, S. Koroyasu, J. Mater. Sci. Tech. **24** (1), 60-64 (2008).

[4] W. Jiang, G. Li, Z. Fan, L. Wang, F. Liu, Metall. Mater. Trans. A, **47** (5), 2462-2470 (2016). DOI: https://doi.org/10.1007/s11661-016-3395-9

[5] G. Li, W. Yang, W. Jiang, F.Guan, H. Jiang, Y. Wu, Z. Fan, J. Mat. Process. Tech. **265**, 112-121 (2019). DOI: https://doi.org/10.1016/j.jmatprotec.2018.10.010

[6] M. M. Hejazi, M. Divandari, E. Taghaddos, Mater. Design. **30** (4), 1085-1092 (2009). DOI: https://doi.org/10.1016/j.matdes.2008.06.032

[7] K.A. Guler, A. Kisasoz, A. Karaaslan, Mater. Test. **56** (9), 737-740 (2014). DOI: https://doi.org/10.3139/120.110625

[8] X. Xiaofeng, Y. Shengping, Y. Weixin, Z. Xiaoguang, X. Qiong, China Foundry. **9** (2), 136-142 (2012).

[9] W. Jiang, Z. Jiang, G. Li, Y. Wu, Z. Fan, Mater. Sci. Tech. **34** (4), 487-492 (2018). DOI: https://doi.org/10.1080/02670836.2017.1407559

[10] A. Akdemir, H. Arikan, R. Kuş, Mater. Sci. Tech. **21** (9), 1099-1102 (2005). DOI: https://doi.org/10.1179/174328405X51785

[11] A. Akdemir, R. Kuş, M. Şimşir, Mater. Sci. Eng. A. **516** (1-2), 119-125 (2009). DOI: https://doi.org/10.1016/j.msea.2009.03.006

[12] A. Avcı, N. Ilkaya, M. Şimşir, A. Akdemir, J. Mat. Process. Tech**. 209** (3), 1410-1416 (2009). DOI: https://doi.org/10.1016/j.jmatprotec.2008.03.052

[13] T. Wróbel, J. Wiedermann, P. Skupień, T. Indian I. Metals. **68** (4), 571-580 (2015). DOI: https://doi.org/10.1007/s12666-014-0488-2

[14] N. Przyszlak, T. Wróbel, A. Dulska, Arch. Metall. Mater. **66** (1), 43-50 (2021). DOI: https://doi.org/10.24425/amm.2021.134757

[15] M. Cholewa, T. Wróbel, S. Tenerowicz, T. Szuter, Arch. Metall. Mater. 55 (3), 771-777 (2010).

[16] N. Przyszlak, T. Wróbel, Archives of Foundry Engineering. **19** (2), 29-34 (2019). DOI: https://doi.org/10.24425/afe.2019.127112

[17] I. Shalevska, P. Kaliuzhnyi, Technology Transfer: Fundamental Principles and Innovative Technical Solutions. 55-57 (2019).